doi:10.1038/nature13186

Connectivity Model Description:

To construct a matrix describing the strength of connection between 213 projection regions approximately tiling the entire brain and defined within the Allen Reference Atlas, we fit a linear connectivity model via constrained optimization, and linear regression.

Figure 4a depicts the connectivity matrix associated with a model of the form:

$$\min_{w_{X,Y}\geq 0} \sum_{i=1}^{|S_E|} \sqrt{\left(\sum_{X \in S_X} w_{X,Y}\, PV(X \cap E_i) - PV(Y) \right)^2}$$

that best fits the data given by the injections in the set S_E. Here S_X is the set of 213 source regions X that project into the target region Y, with *normalized connection strength* $w_{X,Y}$. E_i is the set of all voxels containing neurons infected on the i^{th} injection. The segmented projection volume in an area X is computed by integrating the per-voxel projection density PD (fraction of segmented pixels) across all voxels $v \in X$:

$$PV(X) = \int PD(v)dX$$

Intuitively, $w_{X,Y}$ is a positive or zero number that scales the segmented projection volume in a source region X in order to explain the observed segmented projection volume in a target region Y. For many of the experiments considered, multiple adjacent regions were infected by a single injection; it is possible that several of these source regions project to a given target region. The connectivity model attempts to disentangle this effect by relying on multiple non-overlapping injections to deduce the effective contribution of each region independently. The model that best fitted all anatomical data was found through constrained optimization (2-norm) which seeks a set of positive linear coefficients $w_{X,Y}$ that minimize the difference of projection target regions between the observed values and those generated from the connectivity model. Next, weights found to be identically zero were removed, and a multivariate linear regression determined confidence intervals and p-values on these positive definite weights. Because the same error function is used in both the optimization and the regression, the weights computed by regression were identical to those obtained from optimization.

Only experiments with greater than 75% agreement between informatically labeled injection site voxels and manual annotation of primary and secondary injection structures were included (i.e. 452 of the total 469 experiments). The 213 source regions selected for inclusion in the connectivity model optimization are a subset of the 295 structures included in the raw data connectivity matrix. These regions were selected by simultaneously satisfying 2 criteria: 1) at least one injection experiment that infected a minimum of 50 or more voxels in the region, and 2) using all available data, the selected regions must be “linearly separable” above a predefined

precision, i.e. result in a matrix that is well-scaled for linear analysis, as judged by its conditioning number κ. The first criterion removes structures that might be too small to be informatically aligned during registration, and ensures that there is enough experimental evidence to warrant inclusion as a source region; this resulted in a restriction of the original 295 possible structures to 215 candidate regions. The second criterion was implemented by a greedy algorithm that iteratively added regions to a final list. After each addition, the conditioning number of the resulting matrix (segmented injection volume from each experiment down rows, and regions across columns) was computed, and the next region added that minimally increased this value. This recursive algorithm was continued until the conditioning number reached a predefined threshold ($\kappa = 1000$), and resulted in the exclusion of 2 additional regions to yield a list of 213 regions subsequently analyzed. All analysis data and code are available upon request. The resulting normalized connection strengths and p-values associated with the connectivity matrix in **Figure 4a** are shown in **Supplementary Table 3** as a separate file.

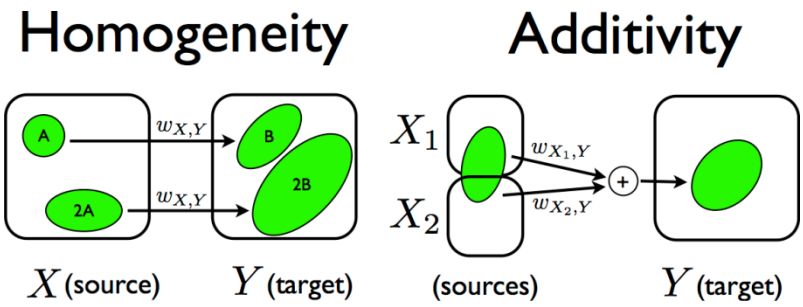

Supplementary Fig. 1: Schematic demonstration of two assumptions necessary to fit the linear connectivity model. Under *homogeneity*, two injections of identical volume into region X result in the same fluorescence in a target region, irrespective of the exact position of the injection within the source area. This assumption is satisfied if the regions are homogenous, but it is also satisfied for topographically organized regions. *Additivity* allows the fluorescence observed in a target region to be explained by a linear sum of appropriately weighted sources.

In practice, if every neuron projecting from a source region were infected, the resulting projection density would saturate the target region. Our model only requires that a subset of the input neurons be infected, so that the measured projection density of the target area is below the saturating nonlinearity. This modeling approach gains a decisive advantage by exploiting, instead of discarding, experimental data with viral tracer in multiple source regions. Data from experiments that infect only a single region can still be utilized in fitting this connectivity model, and can effectively determine isolated individual weights.

The most natural interpretation of the connectivity matrix of **Figure 4a** is as normalized connection strength, describing the amount of segmented signal activated in the target region by infecting one voxel in the source region. In this sense, it can be thought of as proportional to the average out-degree of neurons projecting from the source to the target. An extrinsic notion of connection strength can be obtained by multiplying the normalized connection strength value by the size of the source population; we call this the connection strength, and can be interpreted

as proportional to the total number of axonal fibers projecting from one area to the other. Conversely, an intrinsic notion of connection density can be obtained through division by the size of the target population, approximating the fraction of pixels in a voxel of the target region segmented resulting from infection of all neurons in a single voxel of the source region (and thus less than 1; normalized connection density). Combining these two operations results in a quantity analogous to the fan-in of the source region to the target region, termed connection density; this can be interpreted as the fraction of pixels segmented in a target voxel resulting from infecting the entire source region. These relationships are summarized in **Supplementary Figure 2**.

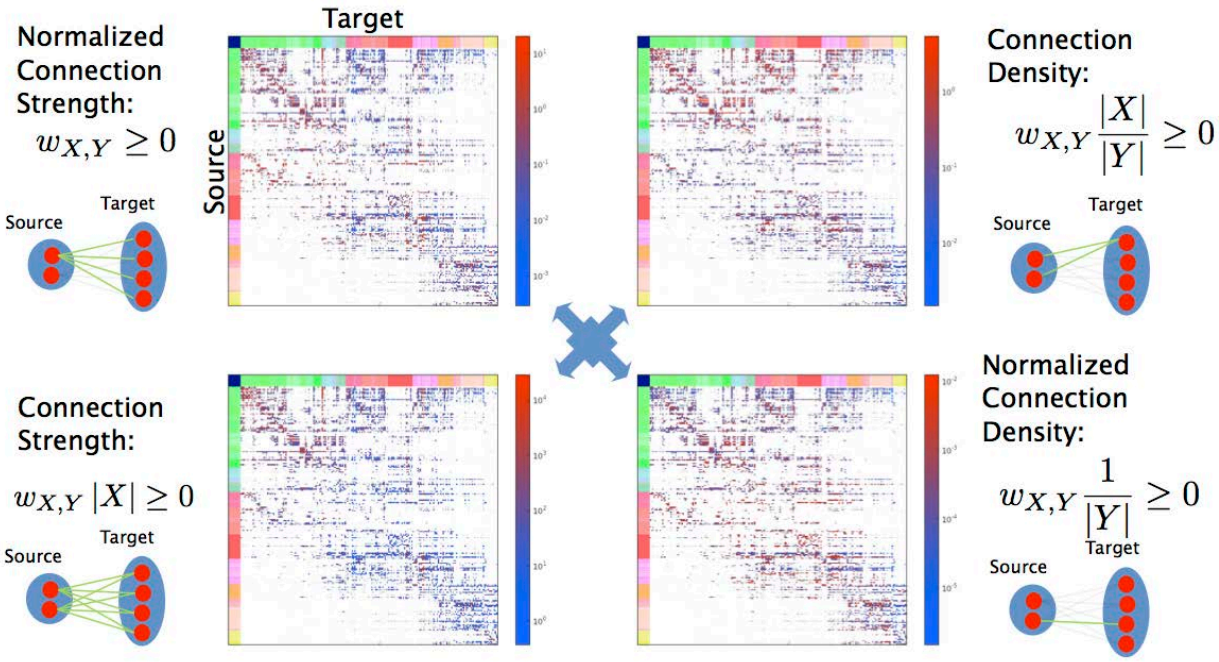

Supplementary Fig. 2: Four notions of inter-region connection strengths. The relative and absolute size of source and target populations can have a significant impact on the inter-region connection strength. The connectivity model results in connection weights best interpreted as normalized connection strength (top-left; see also **Fig. 4a**). Scaling by the size of the source or the target population (or both) can convert between measures.

	Whole Model (ipsi)	Whole Model (contra)	Isocortex (ipsi)	Isocortex (contra)
Optimization	16,954 (37.4%)	15,868 (35.0%)	773 (53.5%)	729 (50.5%)
α = .10	3,529 (7.8%)	2,772 (6.1%)	339 (23.5%)	304 (21.1%)
α = .05	3,123 (6.9%)	2,451 (5.4%)	306 (21.1%)	273 (18.9%)
α = .01	2,487 (5.5%)	1,979 (4.4%)	250 (17.3%)	220 (15.2%)
Low bound	14.1%	11.2%	35.4%	30.0%

Supplementary Table 5: Connection density evaluated after optimization only, and at three levels of statistical significance on the regression p-values, for both the whole model and for isocortical-to-isocortical projections only. Fractions are reported out of 45,369 possible whole-model connections, or 1,444 possible isocortical projections. A low bound for sparsity is estimated as $s_l = 1 - \langle p_i \rangle$.

The connection matrix sparsity (density) can be estimated by using the statistical confidence gained from the regression (**Supplementary Table 5**). Bounded optimization alone results in approximately two-thirds of the possible connections eliminated. A large proportion of the remaining connections have a large p-value associated to them by the subsequent linear regression. In general, cortico-cortical projections are denser than the average density across the entire model. For sparsity, a low bound is estimated by interpreting the regression p value for a connection to be strictly bigger than zero as the probability of a false positive connection $s_l = \sum_{i=1}^{N}(1 - p_i)\,/N$. This represents a low bound of the sparsity, as the probability of false negatives from the optimization cannot be well estimated.

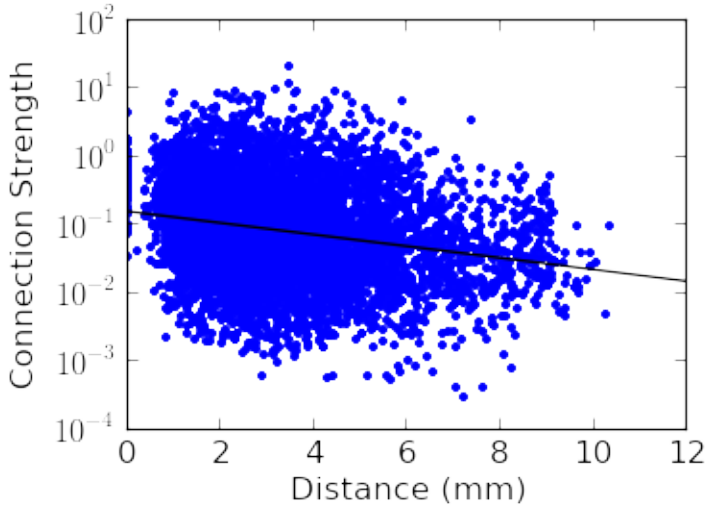

Supplementary Fig. 3: Connection strength negatively correlates with distance. The log of the connection strength between two regions linearly correlates with the distance between the regions, defined as the Cartesian distance between their centers of mass. Only inter-region connections with $p < .05$ are included in the linear regression ($log_{10}s = -0.00854d - 0.793$, r = -0.22, $p < 10^{-16}$). The Cartesian distances between the centers of mass of all the interconnected source and target region pairs are provided in **Supplementary Table 4** as a separate file.

We found that the distribution of whole-brain connection strengths was best fit by a lognormal distribution, based on the Akaike Information Criterion (AIC) which penalizes models with more degrees of freedom (ipsilateral Akaike Information Criterion, AIC: lognormal: -1595.0, inverse Gaussian: -1518.6, exponential: 420.0, normal: 8379.3; lower numbers are more informative), and negatively correlated with the distance between the two regions (**Supplementary Fig. 3**). The best fit normal distribution of the log10 transformed weights has the mean (μ) and standard deviation (σ) of: ipsilateral: μ = -0.94, σ = 0.71, contralateral: μ = -1.26, σ = 0.68; and for only cortico-cortical connections, ipsilateral: μ = -0.54, σ = 0.44, contralateral: μ = -1.0, σ = 0.53 (**Fig. 4b**, red lines). However, after log-transforming the data, the connection distribution failed to pass the Shapiro-Wilk test for normality at α = 0.05 significance level when including all brain regions (ipsilateral: p = 0.039, contralateral: p = 0.023). Because the null hypothesis for this test is normality of the distribution, a significant p value shows significant deviations of the connection distribution from log-normal. After log-transforming, the additional complexity of a two component Gaussian mixture model (GMM) provided an improved ipsilateral distribution: AIC is reduced from 6749.8 to 6747.7. Results were similar for the contralateral connection distribution AIC is reduced from 5090.2 to 5087.8. In both cases, mixture models with additional (>2) components resulted in an increased AIC, and were therefore rejected.

The summary statistics for the GMM models of best fit are provided in **Supplementary Table 6**. Intriguingly, for both ipsilateral and contralateral matrices, one of the mixture components resulting from the fit is close to the cortical distribution (ipsilateral: μ = -0.54, σ = 0.44, contralateral: μ = -1.0, σ = 0.53). This suggests that a mixture of different lognormal distributions of connections, resulting from different regions, might combine together to result in a non-homogeneous distribution of connection weights across the brain.

	Ipsilateral			Contralateral		
	μ	σ	weight	μ	σ	weight
Component 1	-1.33	.62	.48	-1.63	.55	.51
Component 2	-.57	.58	.52	-.88	.60	.49

Supplementary Table 6: Parameters resulting from fitting the log-transformed data from the connectivity weights of each matrix to a 2-component Gaussian mixture model.

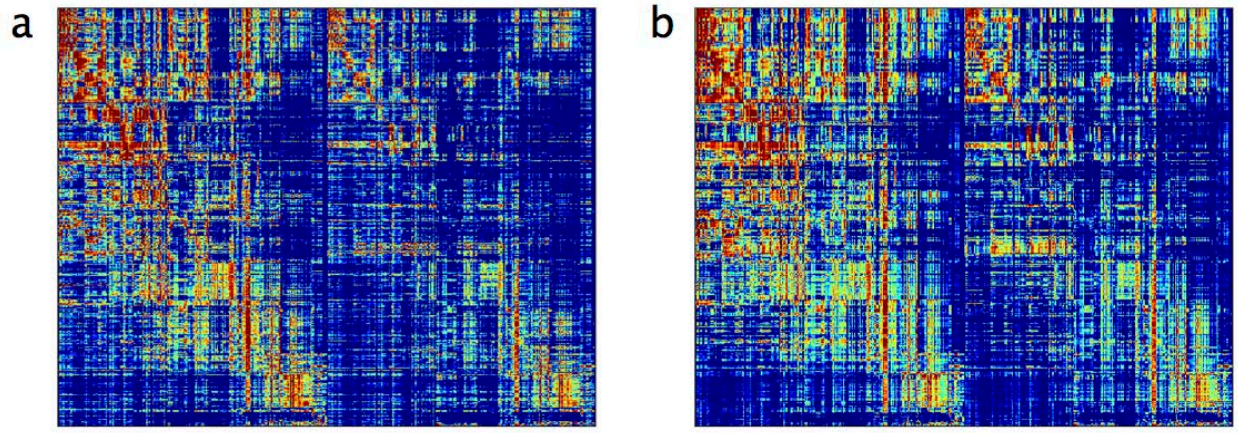

Supplementary Fig. 4: Comparison of normalized projection volume predicted by the linear model with data used for fitting. (**a**) Reproduction of **Figure 3** (main text) restricted to those 213 regions and experiments included in the optimization. (**b**) The prediction of the same data as generated by the linear model, using only the inter-region connectivity matrix and the expression of each injection in the sources.

In order to ascertain the fitting error introduced by the linear optimization model, we computed the expression values predicted by the linear model for each experiment included in the optimization. **Supplementary Figure 4** compares the measured normalized projection volume used to fit the model (a) with the prediction at each target region based on the inter-region connectivity matrix and the measured injection volume in each region in each experiment.

$$NPV_i(Y) = \frac{\sum_{X \in S_X} w_{X,Y}\, PV(X \cap E_i)}{|E_i|}$$

The values of these matrices strongly correlate (Pearson r = .86), implying that the linear model predicts the experimentally observed expression pattern in target regions reasonably well.

Connection Reciprocity:

Previous studies investigated inter-region reciprocity in cortico-cortical connections in rats (Miller and Vogt, 1984; Vogt and Miller, 1983), mice (Wang et al., 2012) and macaque monkey (Felleman and Van Essen, 1991; Markov et al., 2012). However, the relative prevalence of unidirectional versus reciprocal connectivity remains unclear, in part because of a lack of data on connections and strengths in both directions, for a large matrix of brain regions. We addressed this question by applying the weighted, directed, adjacency matrix resulting from the linear model, utilizing the fact that each value of the matrix has a corresponding statistical confidence. We assign each pair of regions a designation as either (i) unconnected, (ii) unidirectionally connected, (iii) reciprocally symmetrically connected, or (iv) reciprocally asymmetrically connected. We define two regions as unconnected if there are no statistically significantly non-zero connections in either direction (as determined by a one-tail z-test at α =

0.05 in each direction). Unidirectional connections are defined as those with only one statistically significant connection. Two regions are defined as reciprocal-symmetrically connected if at least one connection strength is statistically significantly non-zero, and the difference of the two connection strengths fails a two-tail z-test at $\alpha = 0.05$. In contrast, for reciprocal-asymmetric connections, their difference is statistically significant (two-tail z-test at $\alpha = 0.05$).

Among ipsilateral connections, we found comparable numbers of unidirectional connections and reciprocal connections (both asymmetric and symmetric) (1,461 vs. 1,508; **Supplementary Fig. 5**). When the analysis was restricted to the 39 isocortical regions, we found reciprocal connections to be more prevalent (75 unidirectional vs. 156 reciprocal), suggesting that the cortex may be characterized by different connectivity rules, e.g. more reciprocity, than the rest of the brain. Care must be taken in interpreting the results presented in the main text, in light of these definitions of unidirectional and reciprocal connectivity. For example, it is possible to have many fibers from one area to another, and very few (but non-zero) fibers in the opposite direction; here, we define this to be a reciprocal asymmetric connection. To assess the degree to which the disparity between the number of reciprocal and unidirectional connection pairs deviated from chance, we created 100 randomly shuffled connectivity matrices. Using the same criteria as above, we found that the shuffle trials had a greater directionality disparity. We find that although a reciprocal connection does not necessarily follow from a forward projection, it does occur more often than chance, relative to a random matrix with the same entries. However, a note of caution is appropriate here: these connections are characterized between regions, and it is possible that in many reciprocal connections the target of the reciprocal fibers may be a different layer or subregion than the layer or subregion where the direct fibers originated from. Thus the estimate of the fraction of bidirectional connections is an upper bound, and among the bidirectional connections the number of symmetric connections is an upper bound.

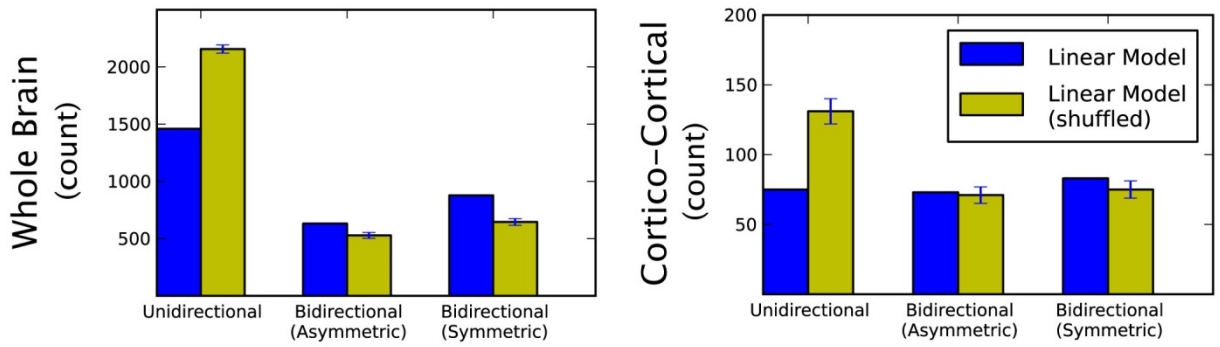

Supplementary Fig. 5: Comparison of reciprocity of ipsilateral connections in which the connection in one direction is significant, and the other is either zero (unidirectional) or nonzero (bidirectional) between all 213 brain regions (left), and between all isocortical regions (right). The bidirectional connections are divided into those in which the two connection weights are significantly different and those which are not.

Graph Analysis:

For each graph type 100 instantiations are generated. For each measure computed, the means and standard deviations over these instantiations are computed and reported as mean (standard deviation). The node clustering coefficient (between 0 and 1) characterizes the tendency of nodes to form tight groups, and is defined as the fraction of triplets made by a node and its neighbors, normalized by the number of such triplets possible. There is a clustering coefficient for each node, and a standard deviation over the nodes in the graph is also reported. Minimum path length represents the length of the path with fewest edges which connect two nodes. The eccentricity of a node represents the distance of the node to the furthest point in the graph. The (in/out) node degree represents the number of edges connecting (to/from) a node, and, by construction, its mean is similar between all graphs. Its standard deviation is important as it characterizes how much variability exists within a graph. The degree centrality is related to node degree by normalization by number of edges.

Name	LM	Shuffled μ	σ	ER μ	σ	WS μ	σ	BA μ	σ
Node	213	210	0.0	210	0.0	210	0.0	210	0.0
Edges	2704	2700	0.0	2700	45	2600	100	2500	89
Density	0.12	0.12	0	0.12	0.0020	0.12	0.0045	0.11	0.0039
Clustering Coefficient (μ)	0.45	0.19	0.0027	0.12	0.0029	0.41	0.010	0.20	0.0075
Clustering Coefficient (σ)	0.13	0.051	0.0040	0.019	0.0010	0.068	0.0034	0.057	0.0051
Minimum Path Length (μ)	2.2	2.0	0.0035	1.9	0.0065	2.1	0.031	2.0	0.016
Minimum Path Length (σ)	0.65	0.45	0.0041	0.39	0.0047	0.59	0.013	0.44	0.010
Eccentricity (μ)	3.4	3.0	0.011	3.0	0.0089	3.0	0.0	2.9	0.019
Eccentricity (σ)	0.49	0.20	0.023	0.11	0.045	0.0	0.0	0.30	0.025
Degree Centrality (μ)	0.12	0.12	0	0.12	0.0020	0.12	0.0045	0.11	0.0039
Degree Centrality (σ)	0.065	0.065	0	0.022	0.0011	0.0095	0.00052	0.067	0.0021
Node Degree (μ)	25	25	0	25	0.43	25	0.95	24	0.84
Node Degree (σ)	14	14	0	4.7	0.23	2.0	0.11	14	0.45
Node In-Degree (μ)	-	-	-	-	-	-	-	-	-
Node In-Degree (σ)	-	-	-	-	-	-	-	-	-
Node Out-Degree (μ)	-	-	-	-	-	-	-	-	-
Node Out-Degree (σ)	-	-	-	-	-	-	-	-	-
In/Out-degree correlation	-	-	-	-	-	-	-	-	-

Supplementary Table 7 characterizes several graph-theoretical parameters computed on a network whose structure is defined by a binarized, undirected version of the connectivity model matrix (LM). Nodes correspond to structures included in the regression of the connectivity model, and edges represent the presence of a statistically significant ($\alpha = 0.05$) directed connection between two regions; the in/out degree of a node is the number of edges into/out of a node (normalizing this number by the size of the network defines the degree centrality of a node). These summary parameters are compared to analogous parameters generated by simulating 1000 realizations of Erdős - Rényi (ER) (Erdős and Rényi, 1960; see Bollobás, 2001), Watts-Strogatz (WS) (Watts and Strogatz, 1998), and Barabási-Albert (BA) (Barabási and Albert, 1999) random graph models, and against 1000 random graphs that are constrained

to have a node distribution identical to LM. An undirected version of the connectivity model is compared the WS and BA models, as these latter models assume undirected edges. To generate the WS random graphs, the mean clustering coefficient was matched to that of LM. For all network parameters, both the mean and standard deviation from realizations of the 1,000 random graphs are reported for both the estimate of the mean and of the standard deviation over the 213 nodes of the graph.

Name	LM, directed	Shuffled μ	σ	ER μ	σ
Node	213	210	0.0	210	0.0
Edges	3123	3100	0.0	3100	64
Density	0.069	0.069	0	0.069	0.0014
Clustering Coefficient (μ)	-	-	-	-	-
Clustering Coefficient (σ)	-	-	-	-	-
Minimum Path Length (μ)	2.9	2.5	0.012	2.3	0.016
Minimum Path Length (σ)	1.1	0.71	0.017	0.58	0.0041
Eccentricity (μ)	4.5	3.5	0.031	3.0	0.024
Eccentricity (σ)	1.0	0.56	0.026	0.18	0.057
Degree Centrality (μ)	0.14	0.14	0	0.14	0.0028
Degree Centrality (σ)	0.076	0.076	0	0.024	0.0011
Node Degree (μ)	29	29	0	29	0.60
Node Degree (σ)	16	16	0	5.2	0.24
Node In-Degree (μ)	15	15	0	15	0.30
Node In-Degree (σ)	5.4	5.4	0	3.7	0.15
Node Out-Degree (μ)	15	15	0	15	0.30
Node Out-Degree (σ)	14	14	0	3.6	0.19
In/Out-degree correlation	0.13	0.13	0	-0.0053	0.071

Supplementary Table 8 The original, directed, version of the connectivity model is compared to the shuffled and ER models.

The node clustering coefficient is defined as the fraction of triplets made by a node and its neighbors, normalized by the number of possible triplets (See Watts and Strogatz, 1998). The eccentricity and minimum path length of a node are complementary views of the maximal and minimal number of edges needed to traverse from one node to another in the graph. We observe that both the undirected (**Supplementary Table 7**) and directed (**Supplementary Table 8**) versions of the connectivity model are incompatible with the ER random graph model. In both cases, the average minimal path lengths between nodes and network eccentricity are significantly different, and the clustering coefficient of the undirected connectivity model is almost four times that of the ER model. A closer agreement is found between the undirected connectivity model and the WS model, where an additional degree of freedom is used to fit the clustering coefficient (the probability of rewiring an edge here set to $\beta = .159$). After this parameter is set, the mean and standard deviation of the minimal path length and degree centrality closely agree. The BA model lacks this additional fit parameter; consequently it cannot fit the clustering coefficient measured in the connectivity model, which takes a smaller value. Similar disagreement holds in all nontrivial measured parameters. Therefore, we

conclude that the undirected version of the connectivity model is more compatible with a Watts-Strogatz small world organization, and less compatible with a Barabasi-Albert scale-free network model.

References:

Barabási and Albert. Emergence of Scaling in Random Networks. Science. 1999.

Bollobás. 2001. Random Graphs (2nd ed.). Cambridge University Press. ISBN 0-521-79722-5

Bullmore and Sporns. Complex brain networks: graph theoretical analysis of structural and functional systems. Nature Reviews Neuroscience. 2009.

Erdős and Rényi. On the evolution of random graphs. Publications of the Mathematical Institute of the Hungarian Academy of Sciences. 1960.

Felleman and Van Essen. Distributed hierarchical processing in the primate cerebral cortex. Cerebral Cortex. 1991.

Markov et al. A Weighted and Directed Interareal Connectivity Matrix for Macaque Cerebral Cortex. Cerebral Cortex. 2012.

Miller and Vogt. Direct connections of rat visual cortex with sensory, motor, and association cortices. The Journal of Comparative Neurology. 1984

Schmitt et al. The Intrinsic Connectome of the Rat Amygdala. Frontiers in Neual Circuits. 2012.

Vogt and Miller. Cortical connections between rat cingulate cortex and visual, motor, and postsubicular cortices. The Journal of Comparative Neurology. 1983.

Wang et al. Network Analysis of Corticocortical Connections Reveals Ventral and Dorsal Processing Streams in Mouse Visual Cortex. The Journal of Neuroscience. 2012.

Watts and Strogatz. Collective dynamics of ‘small-world’ networks. Science. 1998.